

## **Fractional Precipitation of Ni and Co Double Salts from Lithium-Ion Battery Leachates**

### **-Supplement Information**

*John R. Klaehn<sup>1\*</sup>, Meng Shi<sup>1</sup>, Luis A. Diaz<sup>1</sup>, Daniel E. Molina<sup>1</sup>, Reyixiati Repukaiti<sup>1</sup>, Fazlollah Madani Sani<sup>2</sup>, Margaret Lencka<sup>2</sup>, Andre Anderko<sup>2</sup>, Navamoney Arulsamy<sup>3</sup>, Tedd E. Lister<sup>1</sup>*

<sup>1</sup> Critical Materials Institute, Idaho National Laboratory, 2525 Fremont Avenue, Idaho Falls, ID 83402, USA

<sup>2</sup> Critical Materials Institute, OLI Systems Inc., 2 Gatehall Dr., Suite 1D, Parsippany, NJ 07054, USA

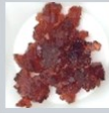










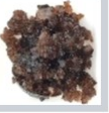



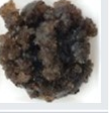

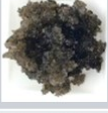







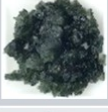







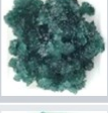










<sup>3</sup> University of Wyoming, 1000 E. University Ave., Laramie, WY 82071, USA

\* Corresponding author, Email: [John.Klaehn@inl.gov](mailto:John.Klaehn@inl.gov)

**Supplemental S1:**

**Tutton's Salt Crystal Formation for Surrogate Leachate Solutions**

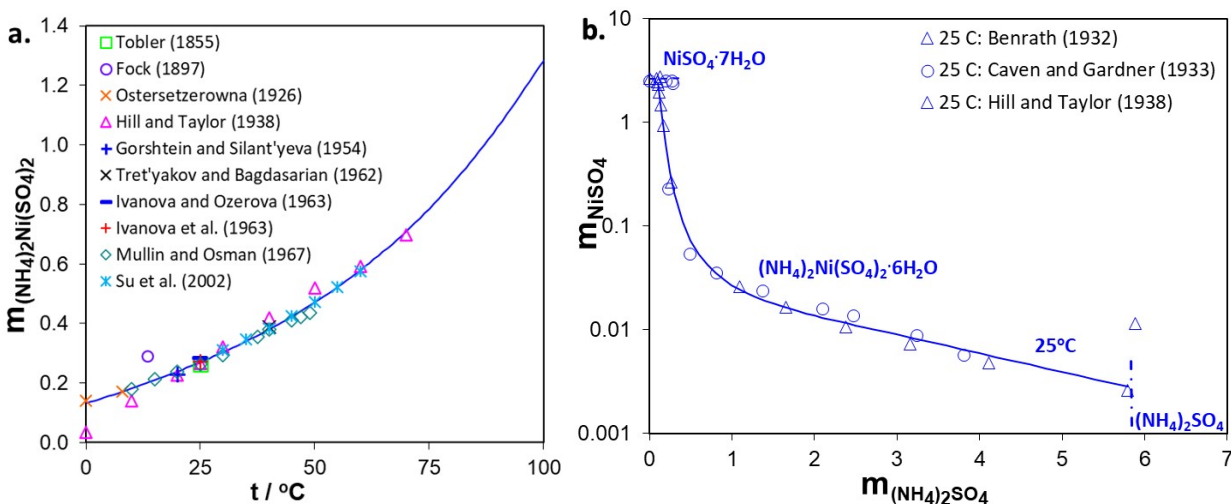
**Table S1.** Comparisons of Tutton's salt formed in surrogate leachate solutions with varying Ni/Co ratios. [see examples from Oliveira (2017), Ghosh (2018), Pacheco (2019), and Villars (2021)]

Temperature /°C	20	20	9	9
(NH <sub>4</sub> ) <sub>2</sub> SO <sub>4</sub> : Ni/Co	1:1	1.5:1	1:1	1.5:1
0% Ni/ 100% Co				
10% Ni/ 90% Co				
20% Ni/ 80% Co				
30% Ni/ 70% Co				
40% Ni/ 60% Co				
50% Ni/ 50% Co				
60% Ni/ 40% Co				
70% Ni/ 30% Co				
80% Ni/ 20% Co				
90% Ni/ 10% Co				
100% Ni/ 0% Co				

## Supplemental S2:

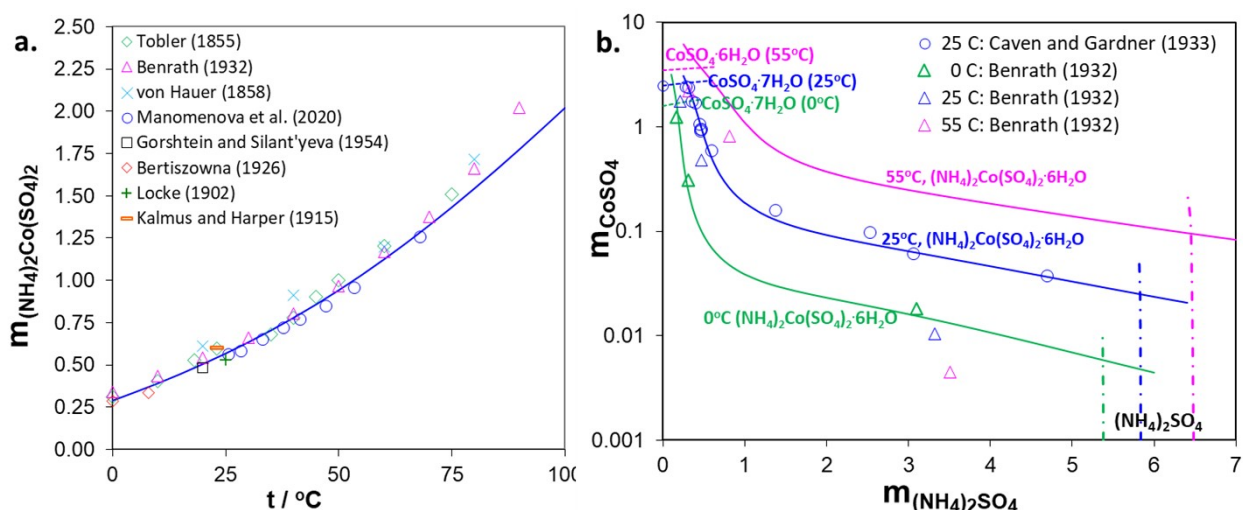
### Validation of the Thermodynamic Model

To validate the MSE thermodynamic model, the solubilities of the sulfates of nickel, cobalt, manganese and lithium in the presence of ammonium sulfate are compared with the available experimental data. All four cations (i.e.,  $\text{Ni}^{2+}$ ,  $\text{Co}^{2+}$ ,  $\text{Mn}^{2+}$ , and  $\text{Li}^+$ ) form double sulfate salts with ammonium cations. In the case of  $\text{Ni}^{2+}$ ,  $\text{Co}^{2+}$ , and  $\text{Mn}^{2+}$ , the dominant crystalline form of the double salt is a hexahydrate. However, the solubilities of these double salts are considerably different. Figure S2-1(a) compares the experimental and calculated solubilities of the double salt  $(\text{NH}_4)_2\text{Ni}(\text{SO}_4)_2 \cdot 6\text{H}_2\text{O}$  as a function of temperature. The experimental data are available from ten different sources and are generally in good agreement at temperatures ranging from 0 °C to 70 °C. The solubility of the double salt increases with temperature from  $\sim 0.14$  m at 0 °C to  $\sim 0.7$  m at 70 °C. In Figure S2-1(b), the concentrations of the two constituent salts, i.e.,  $\text{NiSO}_4$  and  $(\text{NH}_4)_2\text{SO}_4$  are introduced as independent variables at a fixed temperature of 25 °C. It is notable that the hydrated double salt, i.e.,  $(\text{NH}_4)_2\text{Ni}(\text{SO}_4)_2 \cdot 6\text{H}_2\text{O}$ , starts precipitating once as little as  $\sim 0.1$  m  $(\text{NH}_4)_2\text{SO}_4$  is added to a saturated  $\text{NiSO}_4$  solution. The point on the solubility curve when the molalities of both  $\text{NiSO}_4$  and  $(\text{NH}_4)_2\text{SO}_4$  are equal to  $\sim 0.26$  m corresponds to the solubility of the double salt at 25 °C in Fig. S2-1(a). With the addition of ammonium sulfate, the solubility of nickel drops by three orders of magnitude from  $\sim 2.6$  m to as low as 0.0026 m when  $(\text{NH}_4)_2\text{SO}_4$  reaches saturation. The solubility curve of  $(\text{NH}_4)_2\text{Ni}(\text{SO}_4)_2 \cdot 6\text{H}_2\text{O}$  terminates at  $\sim 5.8$  m ammonium sulfate when the latter salt reaches its solubility limit (cf. the vertical dash-dot line in Fig. S2-1(b)). Thus, the addition of ammonium sulfate is a very efficient approach to precipitating nickel as it can reduce the concentration of nickel in solution by as much as three orders of magnitude. The MSE model accurately represents the experimental data.



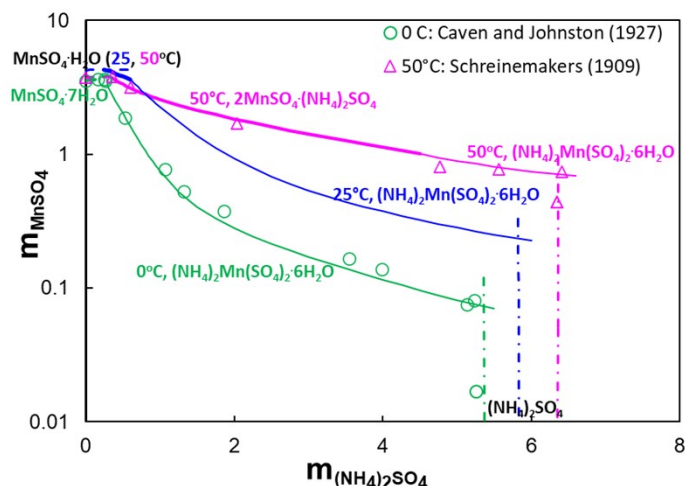
**Figure S2-1.** Calculated (lines) and experimental (symbols) solubility of nickel ammonium sulfate: (a) temperature dependence of the solubility of the double salt  $(\text{NH}_4)_2\text{Ni}(\text{SO}_4)_2 \cdot 6\text{H}_2\text{O}$ ; (b) solid-liquid equilibria in the ternary system  $\text{NiSO}_4 - (\text{NH}_4)_2\text{SO}_4 - \text{H}_2\text{O}$  at a fixed temperature of 25 °C. The lines are calculated with the MSE model.

Figure S2-2 presents an analogous comparison of calculated and experimental solubilities in the ternary system  $\text{CoSO}_4 - (\text{NH}_4)_2\text{SO}_4 - \text{H}_2\text{O}$ . As with nickel, the behavior of this system has been investigated by multiple authors. The solubility patterns of cobalt are qualitatively similar to those of nickel as a similar double salt, i.e.,  $(\text{NH}_4)_2\text{Co}(\text{SO}_4)_2 \cdot 6\text{H}_2\text{O}$  forms upon the addition of ammonium sulfate. The solubility of this double salt also increases with temperature (Fig. S2-2(a)). However, significant quantitative differences are observed. While the solubility of cobalt sulfate is similar to that of nickel sulfate in the absence of ammonium ions (i.e.  $\sim 2.4$  m for  $\text{CoSO}_4$  vs.  $\sim 2.6$  m for  $\text{NiSO}_4$  at  $25^\circ\text{C}$ ), the drop of the solubility upon the addition of  $(\text{NH}_4)_2\text{SO}_4$  is considerably weaker in the case of cobalt. The formation of the double salt leads to a drop in dissolved Co concentration by only about two orders of magnitude (down to  $\sim 0.024$  m when ammonium sulfate reaches saturation at  $25^\circ\text{C}$ ). Nevertheless, the formation of an ammonium-cobalt double sulfate salt remains an effective way of crystallizing cobalt from solution.



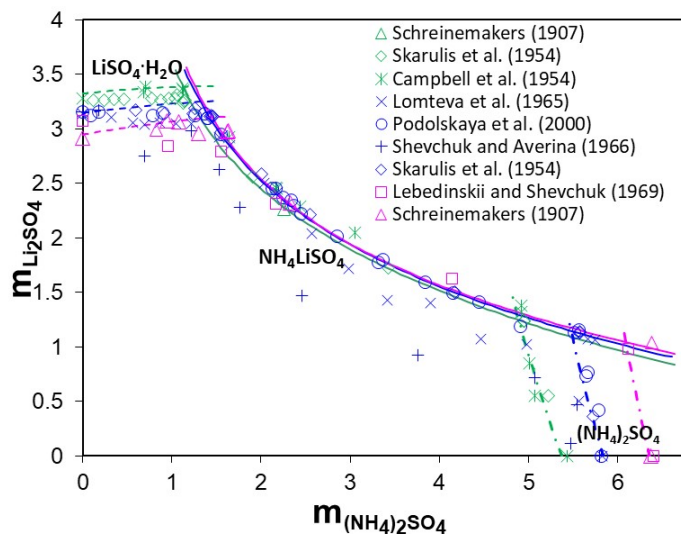
**Figure S2-2.** Calculated (lines) and experimental (symbols) solubility of cobalt ammonium sulfate: (a) temperature dependence of the solubility of the double salt  $(\text{NH}_4)_2\text{Co}(\text{SO}_4)_2 \cdot 6\text{H}_2\text{O}$ ; (b) solid-liquid equilibria in the ternary system  $\text{CoSO}_4 - (\text{NH}_4)_2\text{SO}_4 - \text{H}_2\text{O}$  at fixed temperatures ( $0^\circ\text{C}$ ,  $25^\circ\text{C}$ , and  $50^\circ\text{C}$ ).

The experimental and calculated solubility of manganese in the presence of ammonium sulfate is shown in Figure S2-3. At lower temperatures (i.e.,  $0^\circ\text{C}$  and  $25^\circ\text{C}$ ), manganese forms a double salt that is analogous to those observed for nickel and cobalt, i.e.,  $(\text{NH}_4)_2\text{Mn}(\text{SO}_4)_2 \cdot 6\text{H}_2\text{O}$ . However, this salt is much more soluble than the corresponding nickel and cobalt salts. Upon the addition of ammonium sulfate, the solubility of manganese drops from  $\sim 4.3$  m at  $25^\circ\text{C}$  to  $0.2$  m when ammonium sulfate reaches saturation, which is a considerably higher concentration than that of Ni or Co. Thus, the manganese double salt has a weaker tendency for precipitation compared to the analogous nickel and cobalt salts. Moreover, manganese shows a more complex phase behavior at higher temperatures. At  $50^\circ\text{C}$ , a different double salt, i.e.,  $2\text{MnSO}_4 \cdot (\text{NH}_4)_2\text{SO}_4$  forms at most ammonium sulfate concentrations (cf. the thick purple line in Fig. S2-3) although it transitions to the hexahydrate form at high  $(\text{NH}_4)_2\text{SO}_4$  concentrations, i.e., above  $\sim 4.5$  m.



**Figure S2-3.** Calculated (lines) and experimental (symbols) solid-liquid equilibria in the system  $\text{MnSO}_4 - (\text{NH}_4)_2\text{SO}_4 - \text{H}_2\text{O}$  at three temperatures (0 °C, 25 °C, and 50 °C).

The calculated results and experimental data for lithium sulfate are shown in Figure S2-4. Lithium also forms a double ammonium lithium sulfate salt, but with a different, anhydrous structure, i.e.,  $\text{NH}_4\text{LiSO}_4$ . Unlike in the case of Ni, Co, and Mn, the solubility of this salt is almost independent of temperature in the range from 0 °C to 50 °C (cf. the nearly overlapping green, blue and purple lines in Fig. S2-4). Notably, the solubility of this salt is much higher than those of the Ni, Co and Mn double salts. At 25 °C, the addition of ammonium sulfate results only in a moderate, three-fold reduction of solubility from  $\sim 3.15$  m to  $\sim 1.1$  m at the limit of ammonium sulfate saturation.

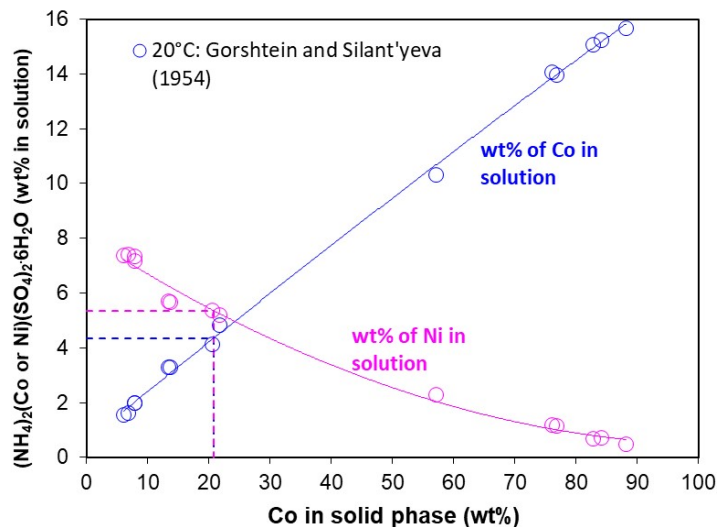


**Figure S2-4.** Calculated (lines) and experimental (symbols) solid-liquid equilibria in the system  $\text{Li}_2\text{SO}_4 - (\text{NH}_4)_2\text{SO}_4 - \text{H}_2\text{O}$  at three temperatures (0 °C – green lines and symbols, 25 °C - blue, and 50 °C - purple).

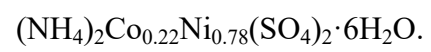


Due to their structural similarity, the cobalt and nickel ammonium double salts form a solid solution in a full range of composition. In general, the solid solution can be represented as  $(\text{NH}_4)_2\text{Co}_x\text{Ni}_{1-x}(\text{SO}_4)_2 \cdot 6\text{H}_2\text{O}$ , where  $x$  ranges from 0 to 1. The solubility of the solid solution was investigated in detail by Gorshtein and Silant'yeva (1954). Figure S2-5 shows the relationship between the composition of the solid solution (expressed as wt% of cobalt relative to the total mass of the metal, Co + Ni, in the solid phase) and the concentrations of both cobalt (blue curve) and nickel (purple curve) in the aqueous solution. It is notable that the relationship between the compositions in the liquid and solid phases is practically linear for Co and nearly linear for Ni. This indicates that the solid solution is reasonably close to ideal with respect to the two end members, i.e.,  $(\text{NH}_4)_2\text{Ni}(\text{SO}_4)_2 \cdot 6\text{H}_2\text{O}$  and  $(\text{NH}_4)_2\text{Co}(\text{SO}_4)_2 \cdot 6\text{H}_2\text{O}$ . The composition of the solid solution identified in this study is denoted by the dotted lines.

The thermodynamic analysis described here indicates that nickel and cobalt can be effectively precipitated from sulfate solutions in the form of hydrated double sulfate salts by adding ammonium sulfate. Since the Ni and Co double salts form a solid solution in the full range of composition, the addition of ammonium sulfate to a mixed nickel – cobalt aqueous system will result in the precipitation of a solid solution. Although the formation of solid solutions containing manganese in addition to nickel and/or cobalt has not been investigated in the literature, such solid solutions are possible due to the structural similarity of the  $(\text{NH}_4)_2\text{Mn}(\text{SO}_4)_2 \cdot 6\text{H}_2\text{O}$  double salt to its nickel and cobalt counterparts. However, the formation of a solid solution is less favored at higher temperatures, at which a different double ammonium manganese double salt, i.e.,  $2\text{MnSO}_4 \cdot (\text{NH}_4)_2\text{SO}_4$  forms (cf. Fig. S2-3). On the other hand, the incorporation of lithium into the solid solution is not expected due to the fact that the ammonium – lithium sulfate double salt has a different structure (i.e.,  $\text{NH}_4\text{LiSO}_4$ ) at all temperatures and its solubility is much higher than that of the Ni, Co, and Mn double salts.



**Figure S2-5.** Solubility of  $(\text{NH}_4)_2\text{Co}_x\text{Ni}_{1-x}(\text{SO}_4)_2 \cdot 6\text{H}_2\text{O}$  solid solutions at 25 °C: Relationship between the concentration of cobalt and nickel in solution as a function of the composition of the solid phase (expressed as weight. % of the metal excluding other elements). The dotted lines indicate the concentrations for the solid solution identified in this study, i.e.,



## Supplemental S3:

### X-ray Crystal Structure Determination

The X-ray diffraction data for  $[\text{NH}_4]_2[\text{Ni}_{0.78}/\text{Co}_{0.22}(\text{H}_2\text{O})_6](\text{SO}_4)_2$  (**1**) [CSD 2361136 contains the supplementary crystallographic data for this paper. These data can be obtained free of charge from The Cambridge Crystallographic Data Centre via [www.ccdc.cam.ac.uk/structures](http://www.ccdc.cam.ac.uk/structures).] were measured at 100 K on a Bruker SMART APEX II CCD area detector system equipped with a graphite monochromator and a Mo  $K\alpha$  fine-focus sealed tube operated at 1.2 kW power (40 kV, 30 mA). A blue prismatic crystal of was glued to a glass fiber using Paratone N oil and the detector was placed at a distance of 5.12 cm from the crystal during the data collection. A series of narrow frames of data were collected at the exposure time of 10 seconds per frame. The frames were integrated with the Bruker SAINT Software package using a narrow-frame integration algorithm. The data were corrected for absorption effects by the multi-scan method (SADABS). Crystallographic data collection parameters and refinement data are collected below in Tables S3-1 through S3-5. Structures were solved by the direct methods using the Bruker SHELXTL Software Package (V. 2017.3-0, Sheldrick, 2015).

All non-hydrogen atoms were located in successive Fourier maps and refined anisotropically. The asymmetric unit contains half of the  $[\text{Ni}/\text{Co}(\text{H}_2\text{O})_6]^{2+}$  cation, a sulfate anion and an ammonium cation. The complex cation is situated on a two-fold symmetry axis, whereas all atoms of the sulfate and ammonium cation are present on general sites (Figure 1). All are well-ordered. The central metal atom of the complex cation is better refined as both Ni and Co occupying the same site with the occupancies of 0.78 and 0.22, respectively. All H atoms were also located in the Fourier maps and were refined isotropically. The H atoms of all of the coordinated water molecules interact with the sulfate anion. Similarly, all four H atoms of the ammonium cation are also H-bonded to the sulfate cation as shown in Figure S3-1. A view of the packing in the crystals is given in Figure S3-2.

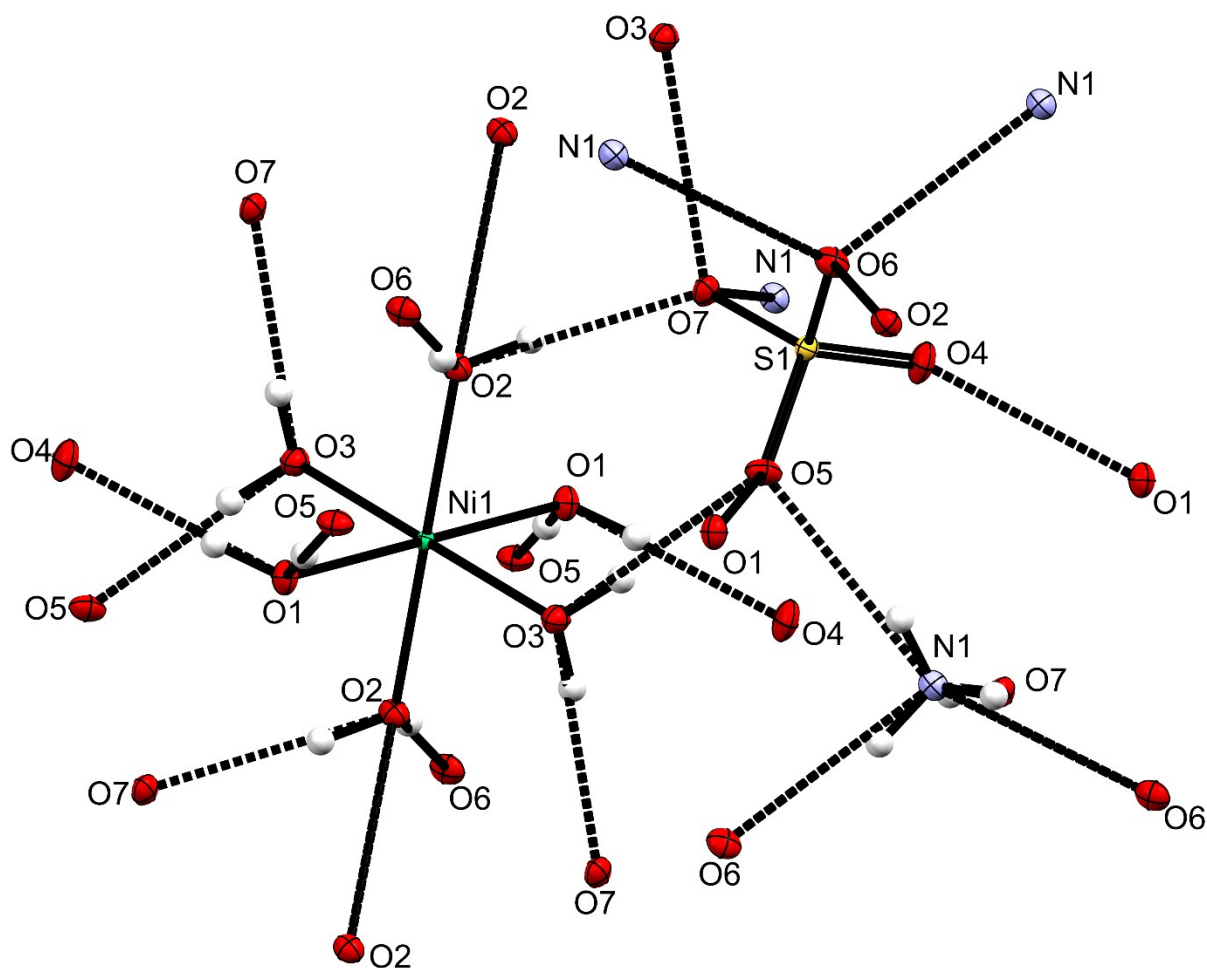
In Figures S3-1 and S3-2, the single crystal X-ray structure reveals a double salt structure (Tutton's salt),  $(\text{NH}_4)_2[\text{Ni}_{0.78}\text{Co}_{0.22}(\text{H}_2\text{O})_6](\text{SO}_4)_2$ . The AA results of the isolated crystals gave metal percentages of Ni and Co (0.78/0.22, respectively) that were applied to the X-ray determination. Crystallographic data and refinement parameters are given in Table 1 (main paper) and the other relevant information, e.g., bond angles and bond lengths (Tables S3-1 to S3-5), are given. For the crystal lattice, none of the atomic bond angles and lengths show any extraordinary variances that were stated in the previous reports. Based on this this crystal determination from the leachate solution, it demonstrates a double salt was formed.

### Software Programs

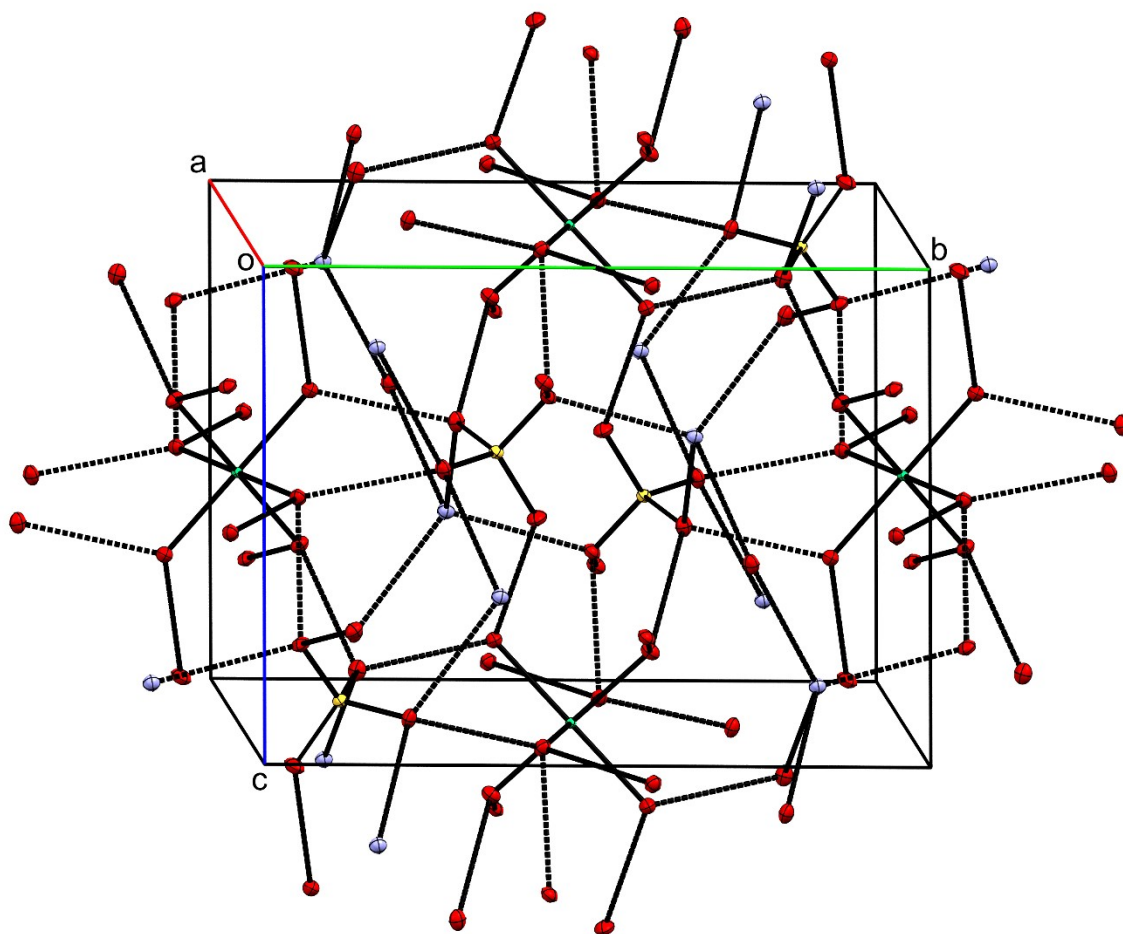
Sheldrick, G.M., 2015. Crystal structure refinement with SHELXL. *Acta Cryst C* 71, 3–8. <https://doi.org/10.1107/S2053229614024218>

Computer programs: Apex3 v2017.3-0, , Bruker AXS Inc.: Madison, WI (Bruker, 2017)





**Figure S3-1.** Hydrogen bonding interactions in  $[\text{NH}_4]_2[\text{Ni}/\text{Co}(\text{H}_2\text{O})_6](\text{SO}_4)_2$ . The smaller component of the central metal ion (Co) is not shown. The thermal ellipsoids are drawn at 50% probability and the hydrogen bonding interactions are represented by solid broken lines.



**Figure S3-2.** Packing in the crystals of  $[\text{NH}_4][\text{Ni}/\text{Co}(\text{H}_2\text{O})_6]_2(\text{SO}_4)$ . All H atoms are omitted and all atoms are unlabeled for clarity. The hydrogen bonding interactions are represented by solid broken lines.

**Table S3-1.** Atomic coordinates ( $\times 10^4$ ) and equivalent isotropic displacement parameters ( $\text{\AA}^2 \times 10^3$ ) for  $(\text{NH}_4)_2[\text{Ni}_{0.78}\text{Co}_{0.22}(\text{H}_2\text{O})_6]$ .  $U(\text{eq})$  is defined as one third of the trace of the orthogonalized  $U^{ij}$  tensor.

	x	y	z	$U(\text{eq})$
Ni(1)	5000	5000	0	4(1)
Co(1)	5000	5000	0	14(1)
O(1)	4649(1)	6123(1)	1599(1)	10(1)
O(2)	2010(1)	4332(1)	-13(1)	10(1)
O(3)	3375(1)	6067(1)	-1725(1)	10(1)
S(1)	2360(1)	3679(1)	4114(1)	7(1)
O(4)	2857(1)	4325(1)	5523(1)	14(1)
O(5)	4444(1)	3249(1)	3870(1)	11(1)
O(6)	878(1)	2758(1)	4216(1)	11(1)
O(7)	1164(1)	4363(1)	2788(1)	10(1)
N(1)	8533(1)	3422(1)	6368(1)	10(1)

**Table S3-2.** Bond lengths [Å] and angles [°] for (NH<sub>4</sub>)<sub>2</sub>[Ni<sub>0.78</sub>Co<sub>0.22</sub>(H<sub>2</sub>O)<sub>6</sub>].

---

Ni(1)-O(2)	2.0405(5)
Ni(1)-O(2)#1	2.0405(5)
Ni(1)-O(1)	2.0677(5)
Ni(1)-O(1)#1	2.0677(5)
Ni(1)-O(3)	2.0729(5)
Ni(1)-O(3)#1	2.0729(5)
Co(1)-O(2)	2.0405(5)
Co(1)-O(2)#1	2.0405(5)
Co(1)-O(1)	2.0677(5)
Co(1)-O(1)#1	2.0677(5)
Co(1)-O(3)	2.0729(5)
Co(1)-O(3)#1	2.0729(5)
O(1)-H(1A)	0.830(14)
O(1)-H(1B)	0.839(15)
O(2)-H(2A)	0.839(15)
O(2)-H(2B)	0.815(14)
O(3)-H(3A)	0.821(15)
O(3)-H(3B)	0.780(15)
S(1)-O(4)	1.4643(5)
S(1)-O(5)	1.4825(5)
S(1)-O(7)	1.4834(5)
S(1)-O(6)	1.4853(5)
N(1)-H(1N)	0.850(15)
N(1)-H(2N)	0.787(16)
N(1)-H(3N)	0.807(16)
N(1)-H(4N)	0.794(17)
O(2)-Ni(1)-O(2)#1	180.0
O(2)-Ni(1)-O(1)	89.34(2)
O(2)#1-Ni(1)-O(1)	90.66(2)
O(2)-Ni(1)-O(1)#1	90.66(2)
O(2)#1-Ni(1)-O(1)#1	89.34(2)
O(1)-Ni(1)-O(1)#1	180.0
O(2)-Ni(1)-O(3)	90.37(2)

O(2)#1-Ni(1)-O(3)	89.63(2)
O(1)-Ni(1)-O(3)	88.86(2)
O(1)#1-Ni(1)-O(3)	91.14(2)
O(2)-Ni(1)-O(3)#1	89.63(2)
O(2)#1-Ni(1)-O(3)#1	90.37(2)
O(1)-Ni(1)-O(3)#1	91.14(2)
O(1)#1-Ni(1)-O(3)#1	88.86(2)
O(3)-Ni(1)-O(3)#1	180.0
O(2)-Co(1)-O(2)#1	180.0
O(2)-Co(1)-O(1)	89.34(2)
O(2)#1-Co(1)-O(1)	90.66(2)
O(2)-Co(1)-O(1)#1	90.66(2)
O(2)#1-Co(1)-O(1)#1	89.34(2)
O(1)-Co(1)-O(1)#1	180.0
O(2)-Co(1)-O(3)	90.37(2)
O(2)#1-Co(1)-O(3)	89.63(2)
O(1)-Co(1)-O(3)	88.86(2)
O(1)#1-Co(1)-O(3)	91.14(2)
O(2)-Co(1)-O(3)#1	89.63(2)
O(2)#1-Co(1)-O(3)#1	90.37(2)
O(1)-Co(1)-O(3)#1	91.14(2)
O(1)#1-Co(1)-O(3)#1	88.86(2)
O(3)-Co(1)-O(3)#1	180.0
Co(1)-O(1)-H(1A)	112.5(9)
Ni(1)-O(1)-H(1A)	112.5(9)
Co(1)-O(1)-H(1B)	115.2(10)
Ni(1)-O(1)-H(1B)	115.2(10)
H(1A)-O(1)-H(1B)	106.2(13)
Co(1)-O(2)-H(2A)	114.1(10)
Ni(1)-O(2)-H(2A)	114.1(10)
Co(1)-O(2)-H(2B)	118.4(10)
Ni(1)-O(2)-H(2B)	118.4(10)
H(2A)-O(2)-H(2B)	105.3(14)
Co(1)-O(3)-H(3A)	117.0(10)
Ni(1)-O(3)-H(3A)	117.0(10)
Co(1)-O(3)-H(3B)	109.7(10)

Ni(1)-O(3)-H(3B)	109.7(10)
H(3A)-O(3)-H(3B)	110.3(14)
O(4)-S(1)-O(5)	110.82(3)
O(4)-S(1)-O(7)	109.40(3)
O(5)-S(1)-O(7)	109.66(3)
O(4)-S(1)-O(6)	109.70(3)
O(5)-S(1)-O(6)	109.16(3)
O(7)-S(1)-O(6)	108.05(3)
H(1N)-N(1)-H(2N)	109.0(14)
H(1N)-N(1)-H(3N)	104.9(14)
H(2N)-N(1)-H(3N)	111.0(15)
H(1N)-N(1)-H(4N)	107.4(14)
H(2N)-N(1)-H(4N)	113.0(16)
H(3N)-N(1)-H(4N)	111.0(16)

---

Symmetry transformations used to generate equivalent atoms:

#1 -x+1,-y+1,-z

**Table S3-3.** Anisotropic displacement parameters ( $\text{\AA}^2 \times 10^3$ ) for  $(\text{NH}_4)_2[\text{Ni}_{0.78}\text{Co}_{0.22}(\text{H}_2\text{O})_6]$ .  
The anisotropic displacement factor exponent takes the form:  $-2\pi^2 [h^2 a^{*2} U^{11} + \dots + 2 h k a^* b^* U^{12}]$

	U11	U22	U33	U23	U13	U12
Ni(1)	5(1)	4(1)	4(1)	0(1)	1(1)	0(1)
O(1)	14(1)	9(1)	9(1)	0(1)	3(1)	0(1)
O(2)	10(1)	9(1)	11(1)	-1(1)	4(1)	-1(1)
O(3)	9(1)	12(1)	10(1)	2(1)	2(1)	0(1)
S(1)	8(1)	7(1)	7(1)	1(1)	1(1)	0(1)
O(4)	20(1)	14(1)	8(1)	-3(1)	1(1)	1(1)
O(5)	9(1)	10(1)	15(1)	1(1)	4(1)	2(1)
O(6)	12(1)	9(1)	14(1)	2(1)	5(1)	-1(1)
O(7)	11(1)	10(1)	8(1)	3(1)	2(1)	2(1)
N(1)	10(1)	10(1)	10(1)	0(1)	4(1)	0(1)



**Table S3-4.** Hydrogen coordinates ( $\times 10^4$ ) and isotropic displacement parameters ( $\text{\AA}^2 \times 10^3$ ) for  $(\text{NH}_4)_2[\text{Ni}_{0.78}\text{Co}_{0.22}(\text{H}_2\text{O})_6]$ .

	x	y	z	U(eq)
H(1A)	5020(20)	6743(11)	1419(15)	20(3)
H(1B)	5380(20)	5986(12)	2511(17)	26(3)
H(2A)	1670(20)	4425(11)	803(17)	26(3)
H(2B)	1810(20)	3688(11)	-207(16)	23(3)
H(3A)	3950(30)	6175(11)	-2412(17)	27(3)
H(3B)	2130(30)	5887(11)	-2072(15)	22(3)
H(1N)	9440(30)	3281(12)	5853(17)	28(3)
H(2N)	8830(30)	3056(13)	7108(18)	34(4)
H(3N)	8730(30)	4055(13)	6590(17)	29(3)
H(4N)	7300(30)	3320(13)	5821(18)	35(4)

**Table S3-5.** Hydrogen bonds for  $(\text{NH}_4)_2[\text{Ni}_{0.78}\text{Co}_{0.22}(\text{H}_2\text{O})_6]$  [ $\text{\AA}$  and  $^\circ$ ].

D-H...A	d(D-H)	d(H...A)	d(D...A)	$\angle(\text{DHA})$
O(1)-H(1A)...O(5)#2	0.830(14)	1.918(14)	2.7420(7)	171.6(13)
O(1)-H(1B)...O(4)#3	0.839(15)	1.849(15)	2.6872(7)	176.2(14)
O(2)-H(2A)...O(7)	0.839(15)	1.927(15)	2.7543(7)	168.6(14)
O(2)-H(2B)...S(1)#4	0.815(14)	3.023(14)	3.8156(6)	164.9(12)
O(2)-H(2B)...O(6)#4	0.815(14)	1.901(14)	2.7096(7)	171.2(14)
O(3)-H(3A)...O(5)#1	0.821(15)	2.012(15)	2.8198(7)	167.7(14)
O(3)-H(3B)...S(1)#5	0.780(15)	2.931(15)	3.6246(6)	149.5(12)
O(3)-H(3B)...O(7)#5	0.780(15)	1.997(15)	2.7696(7)	170.8(14)
N(1)-H(1N)...S(1)#6	0.850(15)	2.791(15)	3.5943(6)	158.1(13)
N(1)-H(1N)...O(4)#6	0.850(15)	2.589(15)	3.2194(8)	131.9(12)
N(1)-H(1N)...O(6)#6	0.850(15)	2.059(15)	2.8884(8)	164.8(14)
N(1)-H(2N)...O(6)#7	0.787(16)	2.213(16)	2.9628(8)	159.4(15)
N(1)-H(3N)...S(1)#3	0.807(16)	2.902(16)	3.6244(6)	150.1(13)
N(1)-H(3N)...O(7)#3	0.807(16)	2.027(16)	2.8291(8)	172.5(15)
N(1)-H(4N)...O(5)	0.794(17)	2.124(17)	2.8918(8)	162.8(16)

Symmetry transformations used to generate equivalent atoms:

#1  $-x+1, -y+1, -z$  #2  $-x+1, y+1/2, -z+1/2$  #3  $-x+1, -y+1, -z+1$

#4  $x, -y+1/2, z-1/2$  #5  $-x, -y+1, -z$  #6  $x+1, y, z$

#7  $x+1, -y+1/2, z+1/2$

## References:

- Bertischówna, B., 1926. Contribution to the problem of solubility of mixed crystals. *Roczniki Chemii* 6, 705-710.
- Campbell, A.N., McCulloch, W.J.G., Kartzmark, E.M., 1954. The system lithium sulfate - ammonium sulfate - water. *Can. J. Chem.* 32, 696-707. <https://doi.org/10.1139/v54-090>.
- Caven, R., Johnston, W., 1927. Equilibrium in the systems  $\text{MnSO}_4\text{-K}_2\text{SO}_4\text{-H}_2\text{O}$  and  $\text{MnSO}_4\text{-(NH}_4)_2\text{SO}_4\text{-H}_2\text{O}$  at  $0^\circ\text{C}$ ; also in the system  $\text{CuSO}_4\text{-Na}_2\text{SO}_4\text{-H}_2\text{O}$  at 0, 25 and  $37.5^\circ\text{C}$ . *J. Chem. Soc.* 2358-2365. <https://doi.org/10.1039/jr9270002358>
- Das, G., Lencka, M.M., Eslamimanesh, A., Anderko, A., Riman, R.E., 2017. Rare-Earth Elements in Aqueous Chloride Systems: Thermodynamic Modeling of Binary and Multicomponent Systems in Wide Concentration Ranges,” *Fluid Phase Equilibria*, 452, 16-57. <http://dx.doi.org/10.1016/j.fluid.2017.08.014>.
- Das, G., Lencka, M.M., Eslamimanesh, A., Wang, P., Anderko, A., Riman, R.E., and Navrotsky, A., 2019. Rare earth sulfates in aqueous systems: Thermodynamic modeling of binary and multicomponent systems over wide concentration and temperature ranges,” *J. Chem. Thermodynamics*, 131, 49-79. <https://doi.org/10.1016/j.jct.2018.10.020>
- Ghosh, S., Oliveira, M., Pacheco, T.S., Perpétuo, G.J., Franco, C.J., 2018. Growth and characterization of ammonium nickel-cobalt sulfate Tutton’s salt for UV light applications. *Journal of Crystal Growth* 487, 104–115. <https://doi.org/10.1016/j.jcrysgro.2018.02.027>
- Gorshtein, G.I., Silant’yeva, N.I., 1954. The distribution of isomorphous and isodimorphous components between solid and liquid phases upon crystallization from aqueous solutions. III. Equilibrium in some systems containing double salts of the schoenite type. *Zh. Obshch. Khim.* 24, 201-203.
- Gruszkiewicz, M.S., Palmer, D.A., Springer, R.D., Wang, P., Anderko, A., 2007. Phase Behavior of Aqueous Na – K – Mg – Ca – Cl –  $\text{NO}_3$  Mixtures: Isopiestic Measurements and Thermodynamic Modeling, *J. Solution Chem.*, 36, 723-765. <https://doi.org/10.1007/s10953-007-9145-2>
- Hill, A.E., Taylor, W.J. Jr., 1938. Ternary Systems. XXIII. Solid Solution among the Picromerite Double Salts at  $25^\circ$ . The Zinc, Copper and Nickel Ammonium Sulfates. *J. Am. Chem. Soc.* 60, 1099–1104. <https://doi.org/10.1021/ja01272a032>
- Ivanova I.N., Ozerova M.I., 1963. Physico - Chemical Analysis. *Sib. Otd. Akad. Nauk SSSR Novosibirsk*, 119.
- Ivanova I.N., Ozerova M.I., Egorova E.I., 1963. Solubility and solid phases in the  $(\text{NH}_4)_2\text{Mg}(\text{SO}_4)_2 - (\text{NH}_4)_2\text{Ni}(\text{SO}_4)_2 - \text{H}_2\text{O}$  system at  $25^\circ\text{C}$ . *Zh. Neorg. Khim.* 8, 977-980.
- Kalmus, H.T., Harper, C., 1915. Physical properties of the metal cobalt. *Ind. Eng. Chem.* 7, 6-17. <https://doi.org/10.1021/ie50073a004>
- Locke, J., 1902. The periodic system and the properties of inorganic compounds. IV. The solubility of double sulfates of the formula  $\text{M}^I_2\text{M}^{II}(\text{SO}_4)_2 \cdot 6\text{H}_2\text{O}$ . *Am. Chem. J.* 27(6), 455-481.
- Lebedinskii, B.N., Shevchuk, V.G., 1969. Solubility in a lithium sulfate-ammonium sulfate-aluminium sulfate-water system. *Ukr. Khim. Zh. (Russ. Ed.)*, 35, 583 in: Sohr, J., Voigt, W., 2017.
- Lomteva, S.A., Kydynov, M.K., Druzhinin, I.G., 1965. Vzaimodeistvie tiomochevini mochevini mineralnimi solyami (Akademia Nauk Kirgizskoi SSR, Bishkek), 38–56.

- Mullin J.W., Osman M.M., 1967. Diffusivity, Density, Viscosity, and Refractive Index of Nickel Ammonium Sulfate Aqueous Solutions. *J. Chem. Eng. Data* 12, 516-517. <https://doi.org/10.1021/je60035a013>
- Oliveira, M. de, Ghosh, S., Pacheco, T.S., Perpétuo, G.J., Franco, C.J., 2017. Growth and structural analysis of ammonium nickel cobalt sulfate hexahydrate crystals. *Mater. Res. Express* 4, 105036. <https://doi.org/10.1088/2053-1591/aa9194>
- Ostersetzerówna D., 1926 About additive properties of mixed crystals. *Roczniki Chemii*, 6, 679-689.
- Pacheco, T.S., Ludwig, Z.M.C., Ghosh, S., Oliveira, V.H., Sant'Anna, D.R., Costa, C.B., Lopes, R., Oliveira, S.O., Saint'Pierre, T.D., Sousa, R.A., Paiva, E.C., 2019. Growth, characterization and vibrational spectroscopy of  $(\text{NH}_4)_2\text{Ni}_x\text{Mn}(1-x)(\text{SO}_4)_2 \cdot 6\text{H}_2\text{O}:\text{Nd}$  crystals. *Mater. Res. Express* 6, 096302. <https://doi.org/10.1088/2053-1591/ab2bbd>
- Podol'skaya, E.P., Khripun, M.K., Rumyantsev, A.V., 2000. *Vestnik of Saint Petersburg University, Ser. 4: Fiz., Khim.* 2, 47 in: Sohr, J., Voigt, W., 2017.
- Scarulis, J.A., Horan, H.A., Maleeny, R., Felten, E., Savino, R., 1954. *J. Am. Chem. Soc.* 76, 3096-3098. <https://doi.org/10.1021/ja01640a085>
- Schreinemakers, F., 1909. Double salts of ammonium sulphate and manganese sulphate. *Chem. Weekblad.* 6, 131-136 in: Sohr, J., Voigt, W., 2017.
- Schreinemakers, F.A.H., 1907. Equilibria in Quaternary Systems. The System: Water, Ethanol, Lithium Sulphate and Ammonium Sulphate. *Zeitschrift für Physikalische Chemie Stochiometrie und Verwandtschaftslehre* 59, 641-669. <https://doi.org/10.1515/zpch-1907-5939>
- Shevchuk, V.G., Averina, R.A., 1966. *Ukr. Khim. Zh. (Russ. Ed.)* 32, 249 in: Sohr, J., Voigt, W., 2017.
- Sohr, J., Voigt, W., 2017. IUPAC-NIST Solubility Data Series. 104. Lithium Sulfate and its Double Salts in Aqueous Solutions. *J. Phys. Chem. Ref. Data* 46, 023101. <http://dx.doi.org/10.1063/1.4977190>
- Tret'yakov U.D., Bagdasarian A.K., 1962. Isothermal Solubility Diagram (at 40°C) of the Quaternary System of Manganese Ammonium Sulfate-Magnesium Ammonium Sulfate-Nickel Ammonium Sulfate-Water. *Zh. Neorg. Khim.* 7, 1716-1723.
- Villars, P., Cenzual, K. (Eds.), 2021. *Crystal Data: Crystal Structure Database for Inorganic Compounds, 2021/22.* ASM International®, Materials Park, Ohio, USA.
- Wang, P., Anderko, A., Young, R.D., 2002. A Speciation-Based Model for Mixed-Solvent Electrolyte Systems. *Fluid Phase Equilibria*, 203, 141-176. [https://doi.org/10.1016/S0378-3812\(02\)00178-4](https://doi.org/10.1016/S0378-3812(02)00178-4)
- Wang, P., Anderko, A., Springer, R.D., Young, R.D., 2006. Modeling Phase Equilibria and Speciation in Mixed Solvent Electrolyte Systems. II. Liquid-liquid equilibria and properties of associating electrolyte solutions" *J. Molec. Liquids*, 125, 37-44. <https://doi.org/10.1016/j.molliq.2005.11.030>
- Wang, P., Anderko, A., Springer, R.D., Kosinski, J.J., Lencka, M.M., 2010. Modeling Chemical and Phase Equilibria in Geochemical Systems Using a Speciation-Based Model, *J. Geochemical Exploration*, 106, 219-225. <https://doi.org/10.1016/j.gexplo.2009.09.003>
- Wang, P., Anderko, A., Kosinski, J.J., Springer, R.D., Lencka, M.M., 2017. Modeling Speciation and Solubility in Aqueous Systems Containing U(IV, VI), Np(IV, V, VI), Pu(III, IV, V, VI), Am(III), and Cm(III) in Wide Concentration Ranges, *J. Solution Chem.*, 46, 521-588. <https://doi.org/10.1007/s10953-017-0587-x>

